Origin of the UG2 chromitite layer, Bushveld Complex

SISIR K. MONDAL AND EDMOND A. MATHEZ*

DEPARTMENT OF EARTH AND PLANETARY SCIENCES, AMERICAN MUSEUM OF NATURAL HISTORY, NEW YORK, NY 10024, USA

Chromitite layers are common in large mafic layered intrusions. A widely accepted hypothesis holds that the chromitites formed as a consequence of injection and mixing of a chemically relatively primitive magma into a chamber occupied by more evolved magma. This forces supersaturation of the mixture in chromite, which upon crystallization accumulates on the magma chamber floor to form a nearly monomineralic layer. To evaluate this and other genetic hypotheses to explain the chromitite layers of the Bushveld Complex, we have conducted a detailed study of the silicate-rich layers immediately above and below the UG2 chromitite and another chromitite layer lower in the stratigraphic section, at the top of the Lower Critical Zone. The UG2 chromitite is well known because it is enriched in the platinum-group elements and extends for nearly the entire 400 km strike length of the eastern and western limbs of the Bushveld Complex. Where we have studied the sequence in the central sector of the eastern Bushveld, the UG2 chromitite is embedded in a massive, 25 m thick plagioclase pyroxenite consisting of 60–70 vol. % granular (cumulus) orthopyroxene with interstitial plagioclase, clinopyroxene, and accessory phases. Throughout the entire pyroxenite layer orthopyroxene exhibits no stratigraphic variations in major or minor elements (Mg-number = 79·3–81·1). However, the 6 m of pyroxenite below the chromitite (footwall pyroxenite) is petrographically distinct from the 17 m of hanging wall pyroxenite. Among the differences are (1) phlogopite, K-feldspar, and quartz are ubiquitous and locally abundant in the footwall pyroxenite but generally absent in the hanging wall pyroxenite, and (2) plagioclase in the footwall pyroxenite is distinctly more sodic and potassic than that in the hanging wall pyroxenite (An_{45-60} vs An_{70-75}). The Lower Critical Zone chromitite is also hosted by orthopyroxenite, but in this case the rocks above and below the chromitite are texturally and compositionally identical. For the UG2, we interpret the interstitial assemblage of the footwall pyroxenite to represent either interstitial melt that formed in situ by fractional crystallization or chemically evolved melt that infiltrated from below. In either case, the melt was trapped in the footwall pyroxenite because the overlying UG2 chromitite was less permeable. If this interpretation is correct, the footwall and hanging wall pyroxenites were essentially identical when they initially formed. However, all the models of chromitite formation that call on mixing of magmas of different compositions or on other processes that result in changes in the chemical or physical conditions attendant on the magma predict that the rocks immediately above and below the chromitite layers should be different. This leads us to propose that the Bushveld chromitites formed by injection of new batches of magma with a composition similar to the resident magma but carrying a suspended load of chromite crystals. The model is supported by the common observation of phenocrysts, including those of chromite, in lavas and hypabyssal rocks, and by chromite abundances in lavas and peridotite sills associated with the Bushveld Complex indicating that geologically reasonable amounts of magma can account for even the massive, 70 cm thick UG2 chromitite. The model requires some crystallization to have occurred in a deeper chamber, for which there is ample geochemical evidence.

INTRODUCTION

Stratiform chromitites are common features of large, layered intrusions. Most mechanisms proposed to account for the chromitites involve changes in chemical or physical conditions that cause the magma to become supersaturated in chromite and remove other phases from the liquidus,

*Corresponding author. Telephone: +1 212-769-5379. Fax: +1 212-769-5339. E-mail: mathez@amnh.org

thus inducing chromite to crystallize and accumulate in monomineralic layers on the magma chamber floor. Among the proposed changes are increases in total pressure (Cameron, 1977; Lipin, 1993), $f\mathrm{O}_2$ (Cameron & Desborough, 1969; Ulmer, 1969), and $a\mathrm{SiO}_2$ (Irvine, 1975). Perhaps the most widely accepted mechanism, however, is that of Irvine (1977a), who proposed that chromitites may form when a chemically primitive magma intrudes into an extant chamber to mix with more evolved magma.

The attraction of the last hypothesis derives from the fact that it is firmly rooted in both phase equilibria and field observations. Thus, Irvine (1977a) showed that in the low-pressure $\mathrm{MgO-Cr_2O_3-SiO_2}$ system the olivine–chromite cotectic is curved such that the mixing of two cotectic liquids of different compositions results in a mixture supersaturated in chromite. He further pointed out that the phase equilibria elegantly explain the stratigraphic sequence peridotite–chromitite–orthopyroxenite observed in the Muskox intrusion. Analogous relations exist in the Stillwater Complex (e.g. Raedeke & McCallum, 1984; Campbell & Murck, 1993) and the Great Dyke (e.g. Wilson, 1992), both of which display a series of cyclic units each ideally constituted by a basal chromitite layer overlain in turn by harzburgite and orthopyroxenite.

Stratiform chromitite layers also exist in the Bushveld Complex. Unlike those in the Stillwater and other intrusions, most of the Bushveld chromitites are immediately underlain and overlain by orthopyroxenite. As originally recognized by Cameron (1980), the existence of chromitite layers in massive orthopyroxenites appears to be inconsistent with Irvine's (1977a) mixing hypothesis. With respect to chromitites, the Bushveld Complex is of interest in another respect, namely, that it contains far more chromite than can be accounted for by the apparent mass of the present body (e.g. Maier & Teigler, 1995; Eales & Cawthorn, 1996; Eales, 2000). This and the relatively low abundance of certain incompatible trace elements of most Bushveld rocks led Cawthorn & Walraven (1998) to postulate that a substantial proportion of the magma had escaped from the chamber as it was filling and crystallizing. Eales (2000) noted the absence of evidence, such as the existence of lavas of the appropriate age and composition, of this lost magma. He went on to propose an alternative solution to the problem whereby some of the magmas that intruded into the Bushveld chamber contained suspended loads of chromite crystals, and that the massive chromitite layers formed by accumulation of these crystals.

Here we take a direct approach to understand the origin of the Bushveld chromitites by conducting a detailed study of the pyroxenite that hosts the UG2 chromitite. This chromitite is of particular interest because it is one of the world's principal platinum-group element (PGE) deposits (the other PGE deposits of the Bushveld are

the Merensky Reef and Platreef), can be traced with only minor interruption along nearly the entire 400 km strike length of the eastern and western lobes of the Bushveld Complex (McLaren & De Villiers, 1982), is well exposed in underground workings and drill core, and has been the subject of several detailed studies. Also included in our investigation is a chromitite layer and its host pyroxenite that are part of Cameron's (1980) E unit, which is the uppermost layer of the Lower Critical Zone.

Our work is based on the study of samples selected from two continuous drill cores (DT-28 and PK-231) through the UG2 unit and one (TW-477) for the E unit. The cores are from the central sector of the eastern Bushveld Complex (Fig. 1). This sector extends $\approx$70 km from the Oliphants River in the north to the Steelpoort fault in the south and is characterized by relative uniformity of the layered rocks along strike.

BUSHVELD CHROMITITES

The Bushveld chromitites occur in the Critical Zone, a stratigraphic interval that in the central sector of the eastern Bushveld is about 800–1000 m thick and has been documented in the classic works of Cameron (Cameron, 1977, 1980, 1982) (Fig. 2). The Lower Critical Zone consists mainly of orthopyroxenite and the Upper Critical Zone of interbedded norite and orthopyroxenite. The existence of chromitite in a stratigraphic interval characterized by a significant proportion of leucocratic rock is in contrast to chromitite occurrences in the Stillwater Complex and Great Dyke, where the chromitite layers are hosted by ultramafic rocks. In the western Bushveld, chromitites form three stratigraphic groupings, traditionally referred to as the lower, middle, and upper groups, with the layers within each group identified by numbers (Cousins & Feringa, 1964) (Fig. 2). Thus, the UG2 is the second layer up-section within the upper group. Except for the UG1, the Upper Critical Zone chromitites are generally embedded in pyroxenite (locally they are underlain by anorthosite). The one that hosts the UG2 is $\approx$25 m thick and is hereafter referred to as the UG2 pyroxenite.

In the central sector of the eastern Bushveld, the UG2 chromitite itself is a massive, 70 cm thick layer consisting of 75–90% modal chromite cemented mainly by plagioclase (Mathez & Mey, 2005). The chromitite is immediately underlain by the so-called mixed layer, which is a 50–70 cm thick unit of chromitite and pegmatoidal plagioclase pyroxenite chaotically mixed on the scales of centimeters to tens of centimeters. The mixed layer in turn is underlain by pegmatoidal plagioclase pyroxenite containing disseminated chromite. The pegmatoid exhibits a sinuous, irregular contact with the underlying pyroxenite, suggesting that the former replaced the latter. Mathez & Mey (2005) argued that the
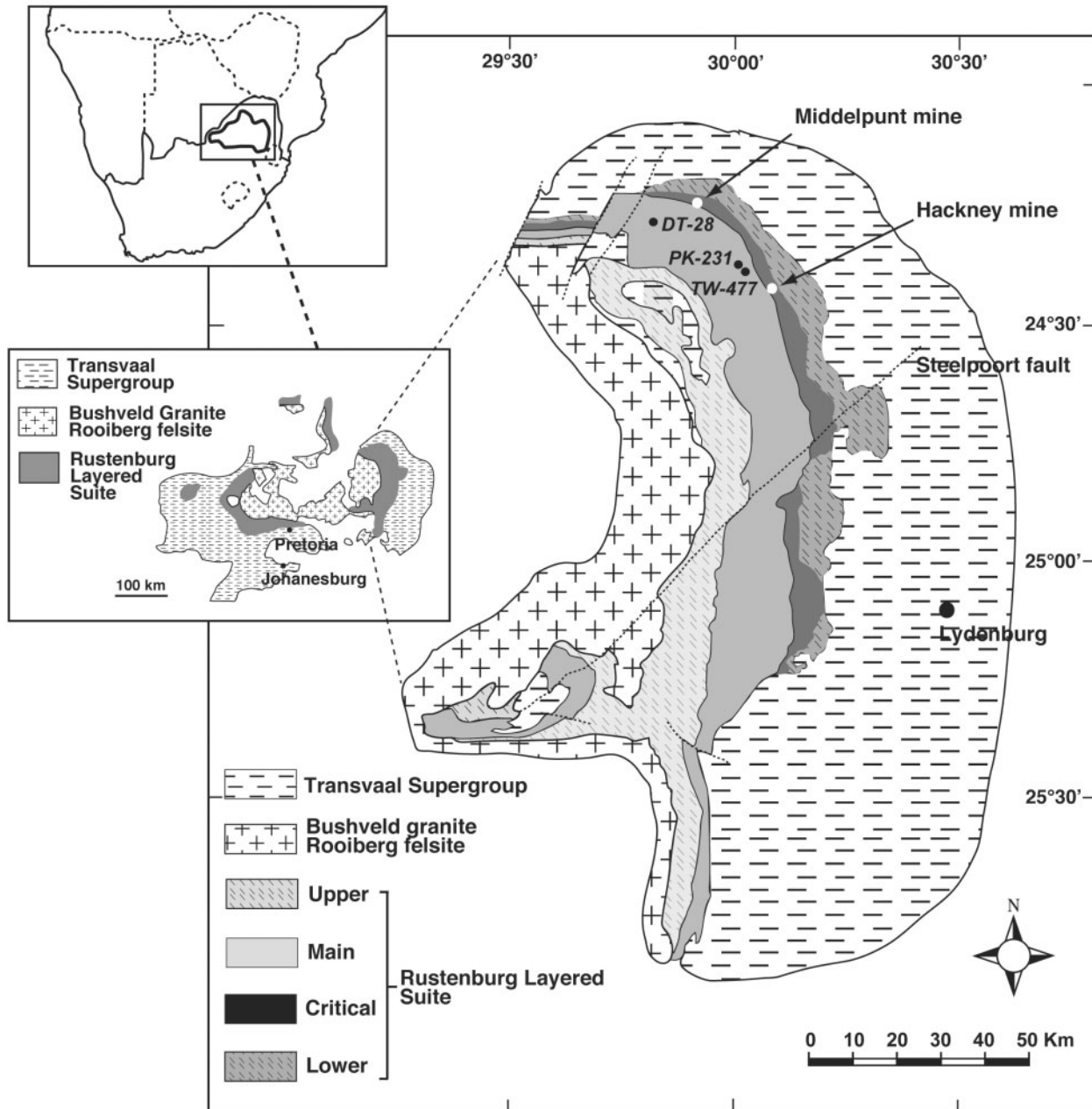
Fig. 1. Generalized geological map of the eastern Bushveld Complex showing locations of the drill cores. Inset maps show the location of the Bushveld Complex in South Africa and the entire Bushveld Complex.

pegmatoidal rocks, which are diagnostic of the UG2, formed when hydrous interstitial melt percolated up through the partially molten crystal pile, ponded beneath a relatively impermeable UG2 chromitite, and metasomatized and partially melted the surrounding rocks, which upon cooling recrystallized to the pegmatoids.

The E unit (Cameron, 1980) is a chromitite-bearing feldspathic pyroxenite (Fig. 2). Three massive chromitite layers, each with thicknesses between 28 and 35 cm and possibly correlative to the MG chromitite layers of the western Bushveld (Hatton & von Gruenewaldt, 1987), commonly occur within the top 7 m of this sequence, although only one is present in core TW-477. This chromitite layer (hereafter referred to as the E chromitite) is 30 cm thick and occurs 2.5 m below the contact between the Upper and Lower Critical Zones and ≈60 m above the Marker chromitite (Cameron, 1980), a prominent 48 cm thick layer of the Lower Critical Zone.
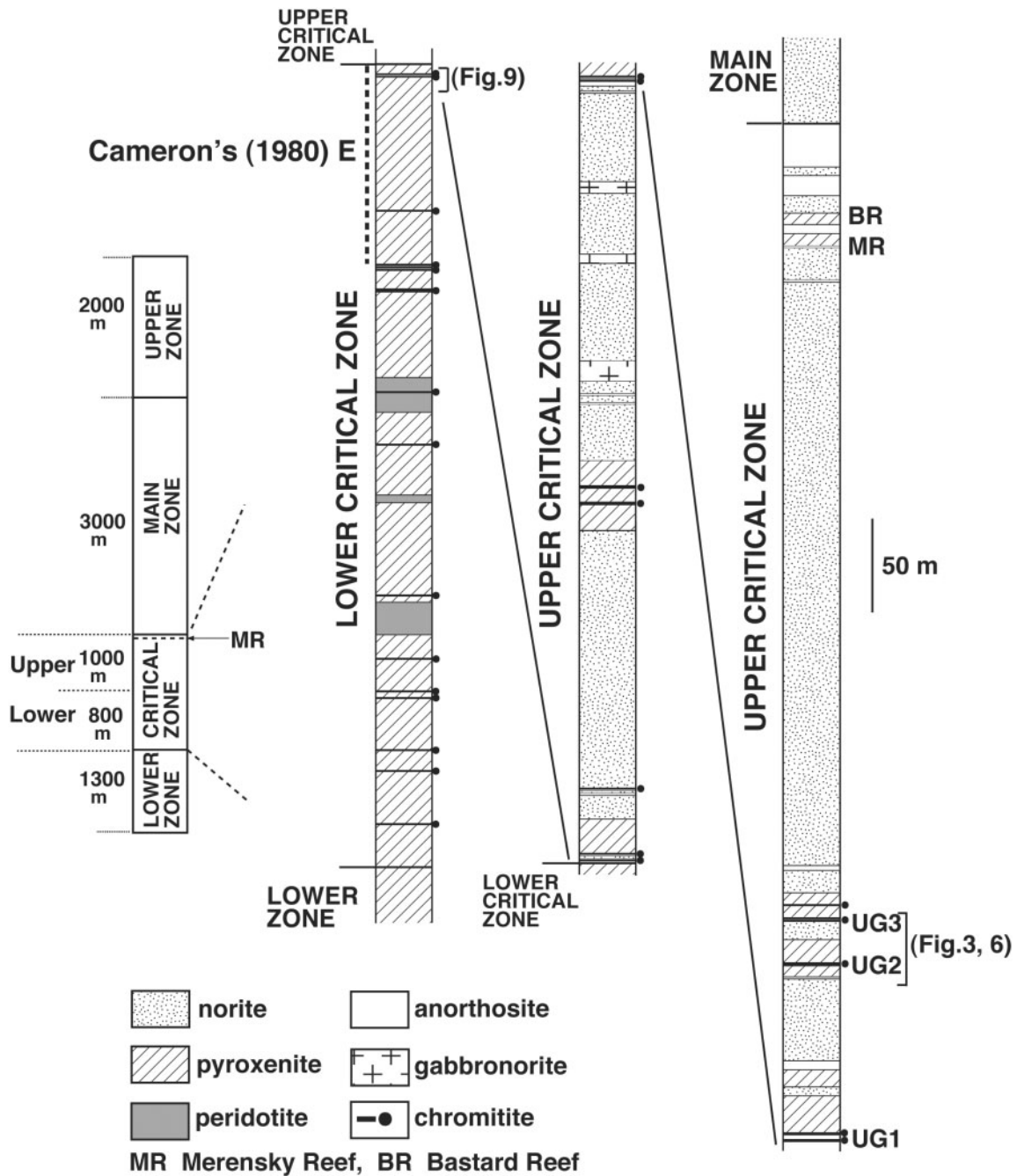
Fig. 2. Generalized litho-stratigraphy of the Critical Zone from the eastern Bushveld Complex (after Cameron, 1980, 1982) showing the studied stratigraphic sections.

THE UG2 PYROXENITE

Petrographic character

The UG2 pyroxenite is a plagioclase pyroxenite consisting of granular (cumulus) orthopyroxene, interstitial plagioclase and clinopyroxene, and minor but variable amounts of phlogopite and other accessory phases. In several respects the pyroxenite below the UG2 chromitite (the footwall pyroxenite) is petrographically distinct from the section above (the hanging wall pyroxenite) (Fig. 3). First, chromite is a minor (up to 4%) but ever-present phase throughout most of the footwall pyroxenite, where it occurs as <0·5 mm in diameter, subhedral to subrounded grains embedded within orthopyroxene and the interstitial phases (Fig. 4a). In the hanging wall pyroxenite, chromite is present within about 2 m of the UG2 chromitite but
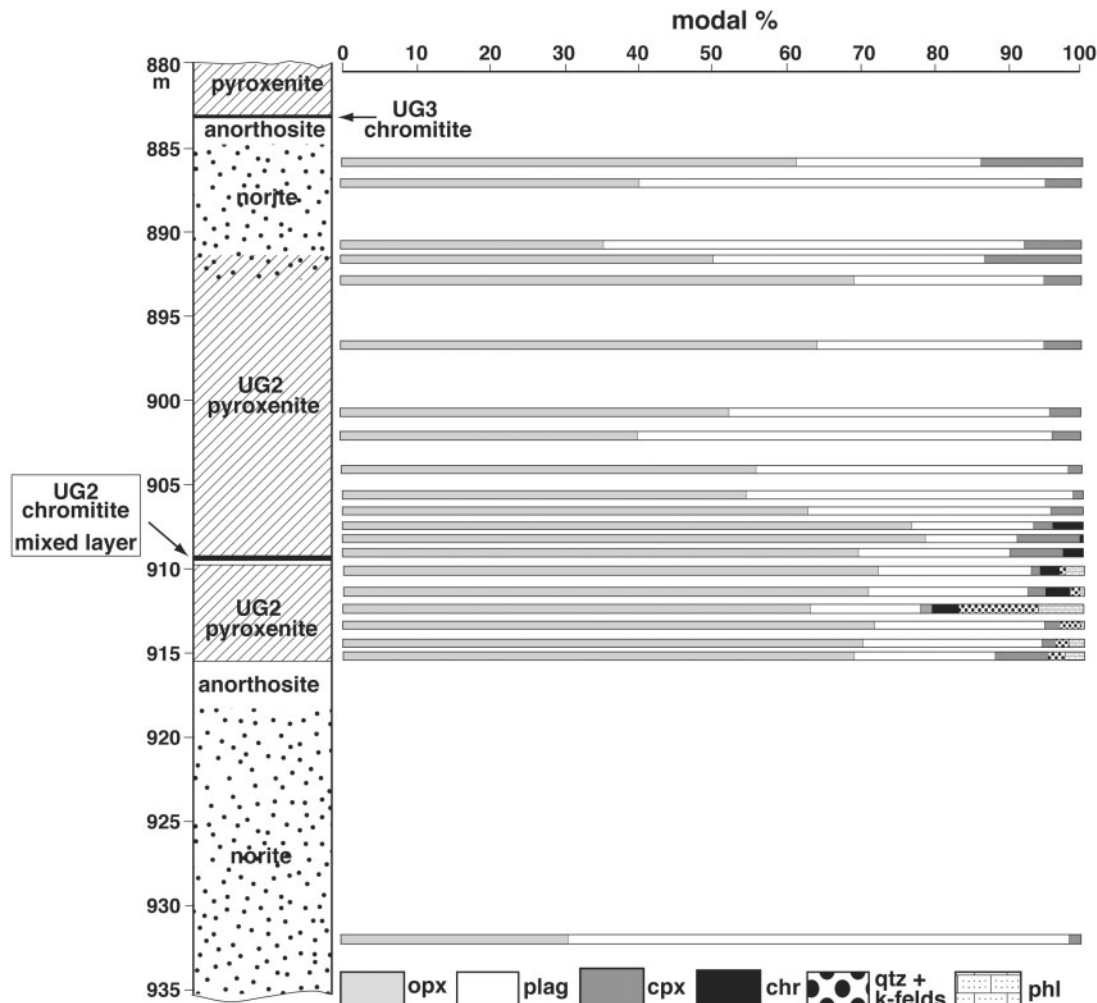
Fig. 3. Rock units and the modal mineralogy of the UG2 sequence as seen in drill core DT-28 from the eastern Bushveld Complex. The modes were determined by point counting (minimum 450 points) of individual thin sections. opx, orthopyroxene; plag, plagioclase; cpx, clinopyroxene; chr, chromite; qtz + k-felds, quartz + K-feldspar; phl, phlogopite. The scale on the left refers to metres below the surface.

completely absent from the rocks above. Second, in the footwall pyroxenite clinopyroxene commonly exists as isolated, centimeter-sized oikocrysts (Fig. 4b), which, because of their large size, are apparent in outcrop and on mine walls. The hanging wall contains about the same amount of clinopyroxene, but it occurs mostly as isolated coronas on orthopyroxene and as much smaller (<3 mm, Fig. 4c) oikocrysts occupying interstices around orthopyroxene. Third, phlogopite, K-feldspar, and quartz are ubiquitous in the footwall pyroxenite (Fig. 4d–f). In fact, in individual thin sections the modal abundances of phlogopite and of quartz + K-feldspar may be as high as 6% and 11%, respectively (Fig. 3). The hanging wall pyroxenite, however, contains only traces of phlogopite. In the footwall, the three phases, sometimes with quartz and feldspar in myrmekitic intergrowth, commonly occur together with chromite in interstices between the

rock-forming minerals. This micro-assemblage of phlogopite + chromite + K-feldspar + quartz is also a feature of the pegmaotidal pyroxenites at the base of the UG2 and associated with the Merensky Reef (e.g. Mathez *et al.*, 1997). Fourth, the footwall pyroxenite is modally homogeneous, containing about 70% orthopyroxene, whereas the pyroxene mode in the hanging wall varies from about 40 to 70% (average ≈ 55–60%). Because the modal variations are gradational, the leucocratic layers are not distinct and included as part of the pyroxenite.

Lastly, the textures of the footwall and hanging wall rocks are different. In the former, orthopyroxene exists both as subhedral, slightly elongate plates up to 3 mm long and as smaller, more irregularly shaped grains among the larger ones. In the hanging wall, the orthopyroxene grains are distinctly more equant, subhedral to rounded, better sorted, and smaller (typical diameters

are 0·6–1·0 mm, locally up to 1·5 mm). The granular pyroxene grains are embedded in a nearly pure 'anorthosite' matrix of complexly intergrown plagioclase grains with variable sizes from 0·1 to 1 mm. In many of the hanging wall rocks plagioclase also exists as rounded, slightly elongate to lath-shaped, 0·1 mm size inclusions (chadacrysts) in both orthopyroxene and interstitial clinopyroxene (Fig. 4c). Despite the distinct difference in grain size and shape, the matrix and chadacryst plagioclase have the same composition. Similar rocks have been found elsewhere in the Critical Zone (Cameron, 1982; Maier & Eales, 1994).

Like practically all rocks of the Bushveld Complex, the UG2 pyroxenite has been partially recrystallized. For example, the mutual contacts of orthopyroxene grains commonly meet at an angle of 120°, and some pyroxene grains appear to have engulfed small plagioclase grains by post-accumulation enlargement (Fig. 5a). Also, the hanging wall pyroxenite locally includes well-foliated rocks. The foliation is defined by subparallel alignment of elongated laths of plagioclase and slender crystals of pyroxene up to 3 mm long (Fig. 5b). We interpret the slender pyroxene crystals to have grown by coalescence of equant grains during a near-solidus shearing event.

Finally, the drill core samples are remarkably fresh. Secondary alteration is limited to rare veinlets of one or more of the minerals talc, serpentine, sericite, and chlorite, and to rare rims of magnetite on disseminated chromite. Base metal sulfide minerals (mainly chalcopyrite) are also rare in the UG2 pyroxenite and generally associated with the alteration assemblage.

Mineral compositions

Constituent phases of the pyroxenites were analyzed by electron microprobe using a Cameca SX100 instrument operated at 15 kV acceleration potential and 20 nA beam current, using natural mineral standards and standard ZAF matrix corrections. The complete dataset is provided as an Electronic Appendix, which can be downloaded from http://www.petrology.oxfordjournals.org.

The data reveal that orthopyroxene and clinopyroxene compositions, in terms of both major and minor elements, are essentially constant throughout the UG2 pyroxenite (Fig. 6). The Mg-number of orthopyroxene ranges from 79·34 to 80·11 ($En_{77.9}Fs_{19.3-20.3}Wo_{1.9-2.8}$) in the footwall and from 79·92 to 81·14 ($En_{77.7-79.8}Fs_{18.6-19.5}Wo_{1.6-2.8}$) in the hanging wall pyroxenite, whereas clinopyroxene compositions are $En_{45.7-50.0}Fs_{8.1-10.4}Wo_{39.7-46.3}$ in the former and $En_{45.6-49.0}Fs_{7.0-9.1}Wo_{41.9-47.4}$ in the latter. These compositions are essentially identical to those of the pyroxenes in the norites above and below the UG2 pyroxenite (Fig. 6). In the UG2 chromitite, orthopyroxene has an Mg-number ≈89, presumably because the orthopyroxene

re-equilibrated with the much larger mass of surrounding chromite during cooling (Mathez & Mey, 2005). In the anorthosite immediately beneath the UG3 chromitite, the pyroxenes are much more Fe-rich than the pyroxenes in the underlying norite or pyroxenite (Fig. 6), a common characteristic of other Bushveld anorthosites (e.g. Eales, 1987; Mathez et al., 1997).

In contrast to pyroxene, plagioclase in the footwall pyroxenite is distinctly more sodic and potassic than that in the hanging wall pyroxenite (Figs 6 and 7). The difference in plagioclase composition is not reflected by a similar difference in Al/Si ratio of the coexisting ortho-pyroxene, implying that in the footwall pyroxenite the two phases are not in equilibrium. Footwall clinopyroxene, on the other hand, is slightly enriched in Na (as reflected in slightly elevated Na/Ca ratio) (Fig. 6). Otherwise, plagioclase displays a uniform composition through the entire sequence studied [except in the UG2 chromitite, where the composition ranges from An_{64} to An_{68} (Mathez & Mey, 2005)].

Compositions of accessory phlogopite in the footwall pyroxenite are presented in Fig. 8. Whereas the Mg-number is uniform through the sequence, the F and Cl contents of phlogopite decrease smoothly upward. The compositions presumably reflect those of the final interstitial melts with which the phlogopite equilibrated. Fluorine and Cl are both incompatible, so their concentrations will increase in residual melt as crystallization proceeds. Therefore, we interpret the profile to be due to an increasing proportion of progressively less chemically evolved interstitial melt upward through the footwall pyroxenite.

The stratigraphic variations in plagioclase composition and modal abundance of phlogopite and quartz + K-feldspar displayed by the footwall pyroxenite in drill core DT-28 (Figs 3 and 6) are also present in the ≈ 22 km distant core PK-231, implying lateral continuity of even these subtle stratigraphic variations in the layer.

# THE E UNIT PYROXENITE, LOWER CRITICAL ZONE

The pyroxenites above and below the E chromitite are essentially identical and consist of granular orthopyroxene with interstitial plagioclase and clinopyroxene, making them typical of other Critical Zone pyroxenites. Clinopyroxene occurs as 2–5 mm sized oikocrysts and coronas on orthopyroxene grains, and <0·5 mm diameter grains of chromite are present embedded mostly in the interstitial minerals. In addition to the chromitite layer itself, chromite is concentrated in several layers, for example, at 673 m (Fig. 9), where its mode reaches ≈10%. In these chromite-rich rocks chromite forms a net-texture surrounding granular orthopyroxene.
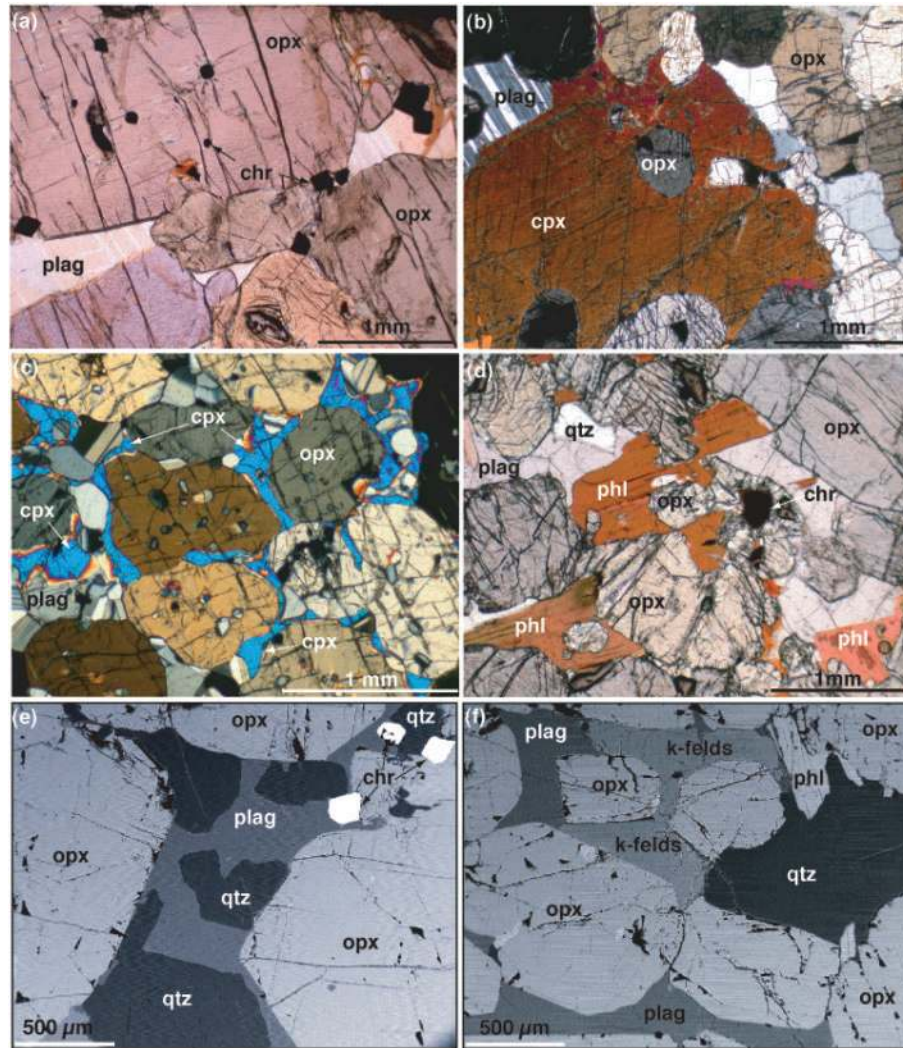
Fig. 4. Photomicrographs illustrating the petrographic character of the UG2 pyroxenite. (a) Sub-rounded to euhedral chromite crystals in granular orthopyroxene and in interstices with plagioclase; plane-polarized light (footwall pyroxenite). (b) Clinopyroxene oikocryst containing rounded chadacrysts of orthopyroxene; crossed nicols (footwall pyroxenite). (c) Plagioclase chadacrysts in granular orthopyroxene and interstitial clinopyroxene; crossed nicols (hanging wall pyroxenite). (d) Accessory quartz along with chromite and phlogopite with plagioclase in interstices between pyroxene grains; plane-polarized light (footwall pyroxenite). (e) and (f) back-scattered electron images of the footwall pyroxenite showing accessory chromite, plagioclase, quartz, K-feldspar and phlogopite in the interstices between pyroxene grains.
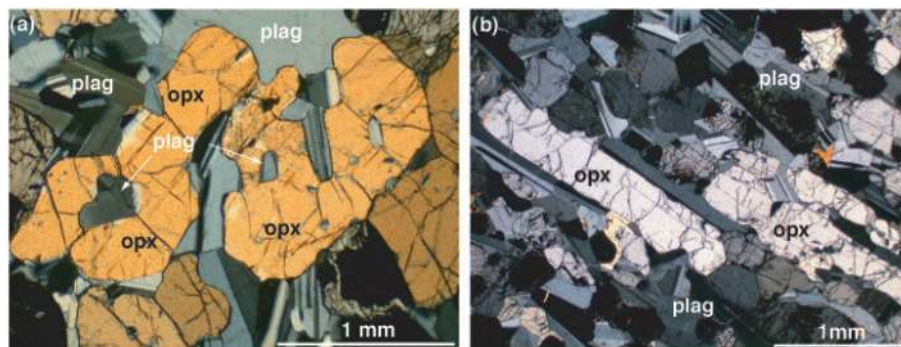
Fig. 5. Photomicrographs showing some characteristics of the UG2 hanging wall pyroxenite. (a) Sintered orthopyroxene engulfing plagioclase grains; crossed nicols. (b) Elongated orthopyroxene and plagioclase crystals aligned parallel to layering; crossed nicols.
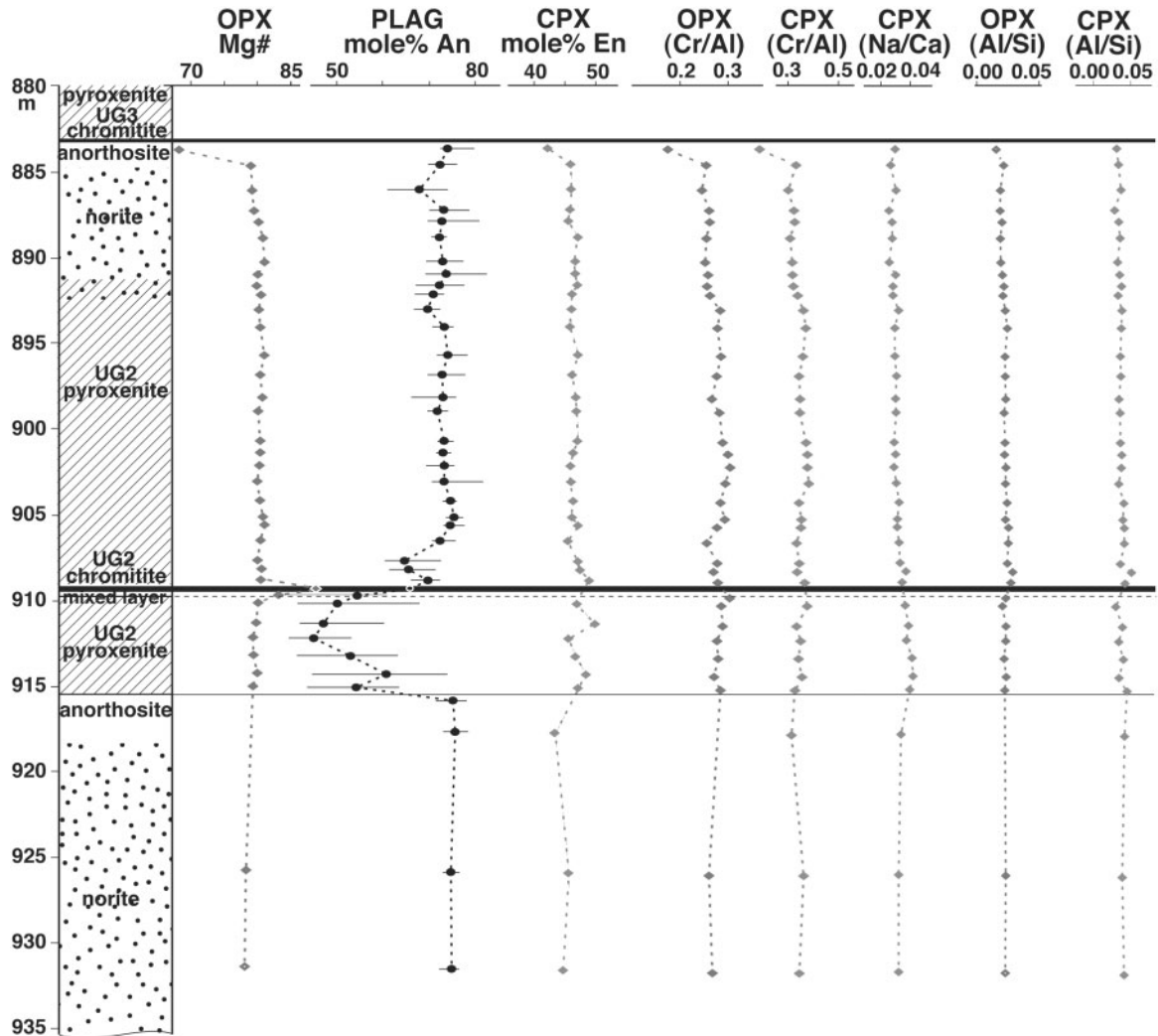
Fig. 6. Mineral composition profiles through the UG2 sequence. Data for the UG2 chromitite are from Mathez & Mey (2005). Horizontal lines indicate compositional ranges; points refer to the averages. Abbreviations as in Fig. 3.

The constituent minerals of four samples from the footwall and three from the hanging wall of the E chromitite have been analyzed. As can be seen in Fig. 9, there are no significant variations in orthopyroxene Mg-number throughout the sequence. On the other hand, pyroxene Cr/Al ratio is sensitive to chromite mode, presumably because of re-equilibration of these phases during cooling; interstitial plagioclase exhibits minor compositional variability.

PETROGENESIS

Petrological evolution of the UG2 footwall pyroxenite

The UG2 footwall pyroxenite is clearly unusual in that (1) whereas the composition of orthopyroxene is constant throughout the section, the composition of the coexisting interstitial plagioclase is variable and more sodic (and potassic) than in the rocks above or below, and (2) the unit contains anomalously high abundances of quartz, phlogopite, and K-feldspar. It is difficult to imagine that these features reflect a changing composition of the magma from which the minerals had accumulated, as the composition of only the interstitial mineral assemblage changes, and it would require that magma Fe/Mg ratio remained constant whereas silica, alumina, and alkali activities changed during growth of the crystal pile. Also, as already noted, granular orthopyroxene and interstitial plagioclase are not in equilibrium throughout the layer.

Two alternative mechanisms are proposed to account for the character of the footwall pyroxenite. One is that the interstitial mineral assemblage represents crystallized interstitial melt. Let us suppose that the footwall pyroxenite initially consisted of a closely packed layer of granular
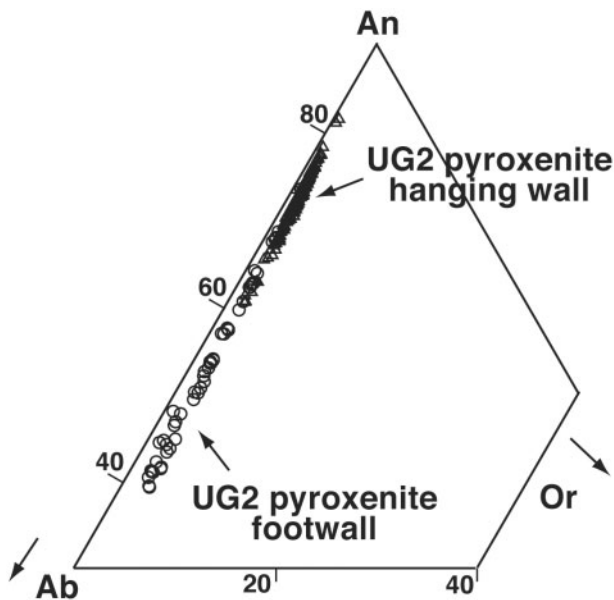
Fig. 7. Compositional ranges of interstitial plagioclase in footwall (○) and hanging wall (△) pyroxenites.

orthopyroxene crystals plus interstitial melt on which was deposited a relatively impermeable layer of chromitite (the present UG2), preventing escape of the melt and thus compaction. To test this idea, we used the MELTS algorithm (Ghiorso & Sack, 1995; Asimow & Ghiorso, 1998) to fractionally crystallize olivine boninite composition U_{1b} of Sharpe *et al.* (1983), a possible parent magma of the ultramafic part of the Bushveld Complex. We first produced an interstitial melt composition by crystallizing U_{1b} at $fO_2 = QFM$ (where QFM is the quartz–fayalite–magnetite buffer) with an arbitrary 1% H_2O added until it reached saturation in orthopyroxene having a composition similar to that of the observed orthopyroxene (En_{80}) and in chromite ($T \approx 1205°C$). We then assumed that the rock consisted of that liquid plus 70% orthopyroxene of En_{80} and allowed the liquid to fractionally crystallize further and in isolation with the En_{80} orthopyroxene, eventually forming K-feldspar and quartz. Crystallization produced plagioclase of An_{56}, which is similar to the observed composition (Fig. 6), and pyroxene of En_{57}. When added to the granular pyroxene, the latter, which amounted to 14% of the initial mass of the liquid, displaced the bulk orthopyroxene composition from En_{80} to $En_{78.9}$. Average footwall orthopyroxene is slightly more Fe-rich than hanging wall orthopyroxene ($En_{80.0}$ vs $En_{80.8}$), so the calculated change in pyroxene composition is consistent with the footwall pyroxenite having formed from a mixture of 70% granular orthopyroxene and 30% interstitial melt that fractionally crystallized *in situ*.

The alternative explanation is that the footwall pyroxenite owes its character to metasomatic infiltration of a chemically evolved interstitial melt, which was trapped there by the overlying, relatively impermeable UG2 chromitite. In this interpretation, metasomatism occurred when the footwall pyroxenite was nearly fully compacted and resulted only in modification of plagioclase composition. The extant localized pockets of K-feldspar, phlogopite, and quartz represent pockets of that evolved melt that had been trapped during the final stages of solidification.

The present observations are not sufficient to distinguish these two models for the post-accumulation evolution of the footwall pyroxenite. Both, however, concern modifications to an initial footwall pyroxenite sequence consisting of orthopyroxene, chromite, and interstitial melt. Because of this and the fact that the composition of orthopyroxene in the footwall and hanging wall pyroxenites is similar, we surmise that the magmas that gave rise to them were nearly identical.

## Models of chromitite formation

The supposition that the pyroxenites above and below the UG2 and E chromitites were initially similar offers a means of testing models that invoke changes in chemical or physical conditions in the magma to account for the chromitite layers. We consider them in turn.

Magma mixing

There are several ways of mixing two different magmas to bring chromite or chromite plus another phase onto the liquidus. As noted, Irvine (1977a) showed that in the $MgO–Cr_2O_3–SiO_2$ system mixing of a chemically primitive melt on the olivine–chromite cotectic with a more evolved cotectic melt or even one saturated in orthopyroxene may result in a mixture saturated in chromite alone, as a result of the manner in which the olivine–chromite cotectic is curved. However, in the more realistic $CaO–MgO–Al_2O_3–Cr_2O_3–SiO_2$ system, the position, shape, and direction of curvature of the olivine–chromite cotectic are sensitive to melt composition (Irvine, 1977b). As the shape of the cotectic is not well known, it is not possible to quantitatively determine the assemblages or contrasting mineral compositions that would result from this type of mixing. Nonetheless, in the scenario suggested by these studies whereby a primitive magma is injected into a chamber occupied by more evolved liquid, the mixture should be less differentiated than the original magma in the chamber, with the result that the accumulated minerals above the chromitite layer should possess higher Mg/Fe ratios than the corresponding minerals below the layer. The average orthopyroxene compositions of the upper and lower pyroxenites are nearly identical, so mixing of relatively primitive and evolved magmas cannot account for the UG2 chromitite.
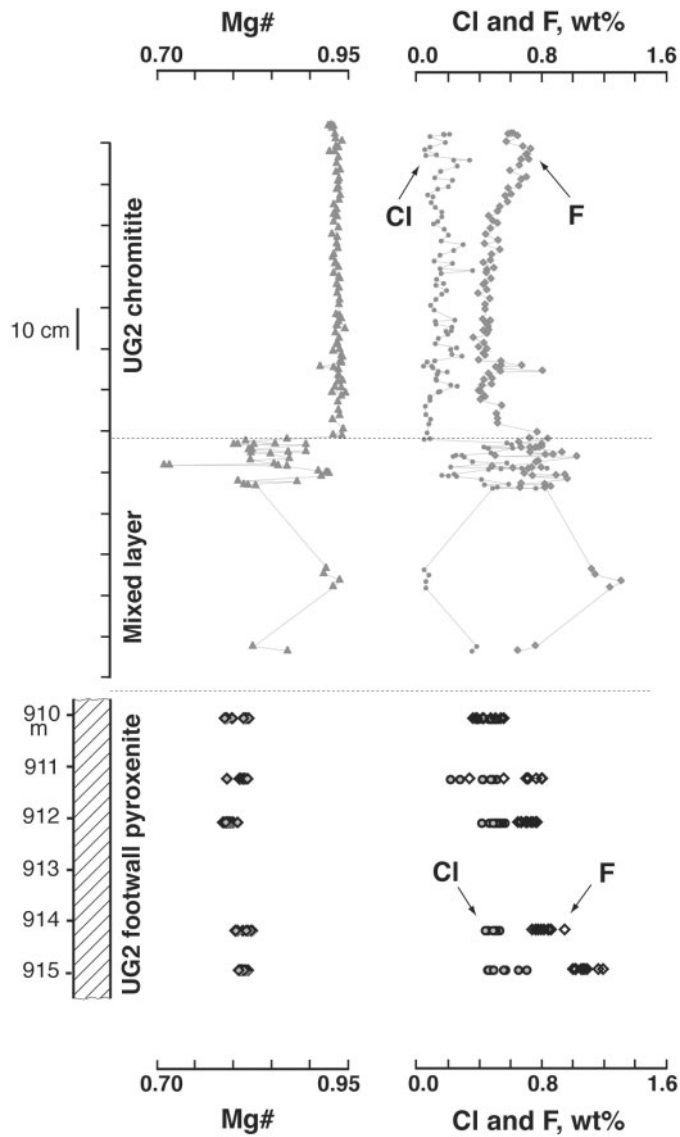
Fig. 8. Variation in phlogopite composition through the UG2 footwall pyroxenite and comparison with phlogopite of the UG2 chromitite and mixed layer (Mathez & Mey, 2005).
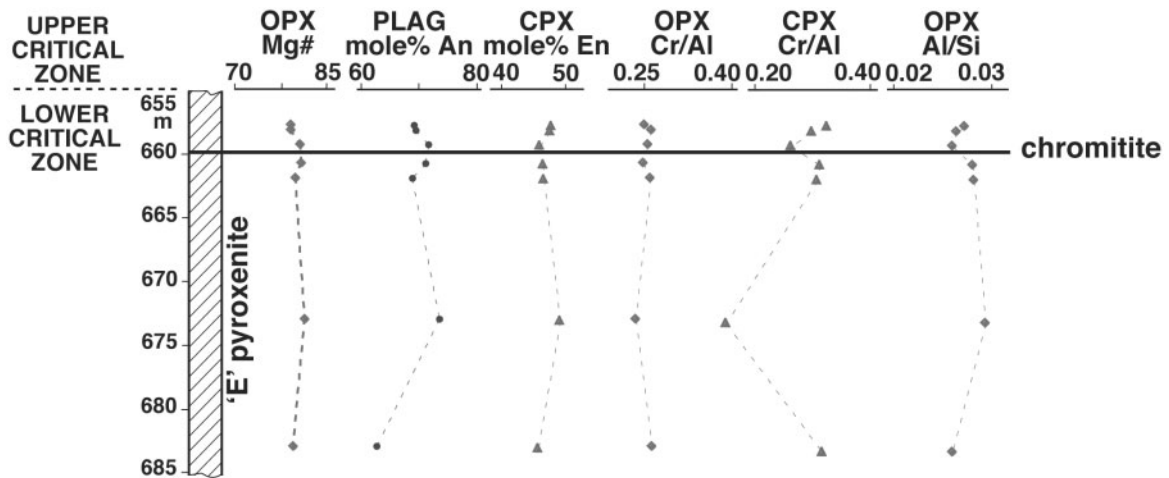
Fig. 9. Mineral composition profiles through the upper part of Cameron's (1980) E unit. Abbreviations as in Fig. 3.

It is also possible to produce chromitite by the mixing of 'U-' and 'A-type' magmas. These are compositionally distinctive magmas inferred by Irvine *et al.* (1983) to produce, respectively, the ultramafic and leucocratic portions of the Stillwater and Bushveld layered sequences. The experiments of Sharpe & Irvine (1983) demonstrated that chromite is the first phase to crystallize from practically all mixtures of their U_{1b} and A_1 compositions. However, the experiments also showed that in most mixtures olivine and chromite are stable together through a large (50°C) temperature interval. Olivine is rare in the Bushveld chromitites and associated rocks. In fact, it is rare throughout the entire Upper Critical Zone, and in the Lower Critical Zone it is restricted mainly to Cameron's (1980) C_1 and C_3 units, which together constitute only 8% of the zone. Furthermore, mixing of A- and U-type magmas should result in the rocks above being different from those below the chromitite layer. Therefore, the formation of the UG2 chromitite by mixing of U- and A-type magmas is not consistent with observations.

Two other possibilities are to mix magmas either possessing different $f O_2$ values (Cameron & Desborough, 1969; Ulmer, 1969) or at different temperatures. A number of experimental studies have demonstrated the strong dependence of chromite stability on these variables (Maurel & Maurel, 1982; Barnes, 1986; Murck & Campbell, 1986; Roeder & Reynolds, 1991) and that, at least in principle, the mixing of melts with different $f O_2$ values or at different temperatures can produce hybrid compositions supersaturated in chromite. However, as there are no indications of any significant changes in the temperature or $f O_2$ of the magma body during formation of the UG2 pyroxenite or the other pyroxenites that host Bushveld chromitites, the amounts of chromite that could reasonably be formed by these processes is small.

Contamination

Irvine (1975) proposed that chromitite layers may have formed by the contamination of mafic magma by silica from digestion of granitic roof rocks. He subsequently rejected the idea, pointing out that the addition of alkalis would shift the olivine–orthopyroxene reaction boundary toward silica such that 'geologically improbable amounts of contamination would be required to induce the crystallization change' (Irvine, 1977a, p. 273). Without reference to this problem, Kinnaird *et al.* (2002) and Spandler *et al.* (2005) used isotopic measurements and observations of mineral inclusions in chromite, respectively, to revive the model.

Spandler *et al.* (2005) reported inclusions in chromite of the Stillwater G chromitite consisting of enstatite + Na-phlogopite ± Na–Ca amphibole ± albite ± diopside. They were able to completely melt some of the inclusions to produce a set of homogeneous glasses with compositional ranges of 45·0–50·6 wt % SiO_2, 14·1–21·0% MgO, 14·7–16·7% FeO, 0·76–1·22% CaO, and 4·5–6·1% Na_2O. They interpreted these to represent the melt compositions from which the chromite crystallized and suggested that the melts formed by mixture of high Mg-basalt and trondhjemite, the latter derived by partial melting of the magma chamber roof. There is general agreement that the so-called 'U-type' magmas believed to be the parents of the lower portions of the Bushveld and Stillwater Complexes were siliceous picrites with SiO_2 contents in excess of 52 wt % (e.g. Davies *et al.*, 1980; Cawthorn *et al.*, 1981; Longhi *et al.*, 1983; Sharpe & Hulbert, 1985). For example, the U_{1b} liquid (Sharpe *et al.*, 1983) contains ≈57% SiO_2, so mixtures of it and more siliceous trondhjemite bear no resemblance to the inclusion compositions. Nonetheless, we investigated the inclusion compositions further using MELTS (Ghiorso & Sack, 1995; Asimow & Ghiorso, 1998). According to MELTS, the inclusion compositions with an arbitrary 1·0 wt % water and 0·05 wt % Cr_2O_3 added possess liquidi in excess of 1450°C and crystallize more forsteritic olivine than is observed in the Stillwater Complex [Fo_{87-90} vs Fo_{82-86} [Raedeke & McCallum, 1984)]. Therefore, we conclude that the inclusions described by Spandler *et al.* (2005) do not represent the magma from which the chromitite originally crystallized. This is in accord with the work of Li *et al.* (2005), who described inclusions similar to those reported by Spandler *et al.* (2005) in chromite from the Merensky Reef. Following Nicholson & Mathez (1991), Li *et al.* (2005) proposed that water-rich fluid driven out of the underlying crystal pile mixed with orthopyroxene-bearing magma to cause resorption of orthopyroxene and crystallization of chromite. In their model, the inclusions represent variable proportions of residual orthopyroxene crystals, hydrous melt, and fluid trapped by the growing chromite. As a final point, mineral inclusions with the general character of those reported by Spandler *et al.* (2005) are common in chromite from chromitites of ophiolites (e.g. Lorand & Ceuleneer, 1989; McElduff & Stumpfl, 1991; Melcher *et al.*, 1997) and are sometimes associated with fluid inclusions.

In an extensive analysis of whole-rock and plagioclase separates, Kinnaird *et al.* (2002) reported that the UG2 chromitite possesses variable and generally higher initial $^{87}Sr/^{86}Sr$ ratios [$(^{87}Sr/^{86}Sr)_i$] than the overlying and underlying silicate-rich rocks. These data add to the generally confusing isotopic signatures of Bushveld (and Stillwater) chromitites. For example, the chromitites exhibit variable Os isotope signatures, a feature that is partly due to the fact that the $(^{187}Os/^{188}Os)_i$ ratios of chromite separates and their corresponding bulk-rocks are commonly different (e.g. Marcantonio *et al.*, 1993; Lambert *et al.*, 1994; McCandless *et al.*, 1999; Schoenberg *et al.*, 1999; Horan *et al.*, 2001). Also, the Pb isotope data of Mathez & Kent

(2005) show that the UG2 chromitite and adjacent rocks contain Pb from at least three distinct sources, and that some of the Pb was introduced after the rock had been at least partially solidified. The basic lesson from Os and Pb isotope studies is that bulk-rock and mineral analyses are not accurate indicators of the composition of the parent magma, and this may be true for Sr as well.

In the case of the UG2 sequence, simple application of the contamination model predicts that the rocks above the UG2 chromitite should be more silica-rich than those below. However, the opposite is true. Another objection to this model (and one that also applies to the magma mixing model) was enunciated by Lipin (1993), who pointed to the difficulty of mixing liquids of markedly different viscosities and densities, especially over the vast distances that would be required to account for the UG2 chromitite.

To test the silica addition model further, we used MELTS to explore the crystallization behavior of composition U_{1b} to which varying proportions of SiO_2 and average Archaean grey gneiss (Martin, 1994) were added. In general, the hybrid magmas first saturated in orthopyroxene and then in chromite, and we were unable to produce a hybrid magma that both reproduced the observed composition of hanging wall orthopyroxene and was initially saturated just in chromite.

Ephemeral pressure increase

Cameron (1977) speculated that an ephemeral pressure increase on the magma could account for the formation of the Bushveld chromitites, and the idea was developed in detail by Lipin (1993). The attraction of this model is that it offers a way to produce a chromitite layer extending for vast distances, as pressure change propagates rapidly. Based on observations from Kilauea, Lipin (1993) estimated that overpressures of 5–10% are possible in magma chambers as a result of the exsolution of vapor. He went on to point to experiments in Cr- and Fe-free systems (Sen & Presnall, 1984) showing that the spinel field of stability increases at the expense of the silicate minerals with increasing pressure. The problem with the model is that neither the phase boundaries involving spinel (Sen & Presnall, 1984) nor the Cr solubility in melt at chromite saturation appear to be even moderately sensitive to changes in total pressure. The only data on Cr solubility at chromite saturation as a function of pressure are from the five experiments of Roeder & Reynolds (1991), which suggest that Cr solubility may actually increase rather than decrease with pressure. Finally, if the UG2 chromitite formed by simply closed-system crystallization of chromite in response to pressure change, the Cr/Al ratio of hanging wall orthopyroxene should be different from that of footwall orthopyroxene, which is not the case. Therefore, a change in pressure to account for the UG2 chromitite is not consistent with the observations.

Addition of water

Nicholson & Mathez (1991) proposed that the thin chromitite seams of the Merensky Reef formed at fronts of hydrous interstitial melt migrating through the crystal pile. The notion was based on experiments [Ford *et al.* (1972), since confirmed by more recent experiments of Sisson & Grove (1993) and Gaetani *et al.* (1994), among others] showing that addition of water to a silicate melt suppresses the crystallization temperatures of all the silicate minerals more than that of chromite. The formation of a chromitite by this mechanism would require dissolution of about 50 times its mass in clinopyroxene and nearly 100 times its mass in orthopyroxene, based on the observed Cr contents of these minerals. In the case of the UG2 chromitite, this would require dissolving all the pyroxene from a partially molten body of rock over 100 m thick and then extracting and concentrating the chromite. It is difficult to imagine a geological situation in which this could happen, let alone one involving the addition of a large mass of water to a large mass of partially molten rock.

Origin of UG2 chromitite

The fact that none of the models considered above adequately accounts for the observed rock sequence leads us to the model of Eales (2000), which holds that the chromitites formed by accumulation of chromite from crystal-charged magmas injected into the Bushveld chamber. Eales (2000) pointed to the basic problem that there is far too much Cr present in chromite and pyroxene than can be accounted for by the column of existing rock, assuming that the present column represents the entire magma mass (i.e. no magma escaped from the Bushveld chamber). For example, based on studies of the section in the northwestern part of the Complex, he determined that the entire 1260 m thick Critical Zone contains $\approx 1\cdot40$ wt % Cr_2O_3. The formation of such a layer would have required in a column of magma containing 0·15 wt % Cr_2O_3 more than 15 km thick, or nearly double the thickness of the layered mafic rock sequence. Exacerbating the problem, he further showed that the magmas that formed the thick Main and Upper Zones of the Complex could not have contributed substantially to the Cr budget of the underlying Critical Zone.

Here we adopt Eales's (2000) model and propose that the UG2 chromitite formed by injection of a new batch of magma containing suspended chromite and orthopyroxene crystals into an extant magma occupying the present fossil chamber. The compositions of the two magmas were approximately similar, as they were both crystallizing orthopyroxene + chromite of similar composition. The chromite from the newly injected magma mechanically separated from the orthopyroxene and rapidly accumulated and spread out to form a dense,

monomineralic, and relatively impermeable layer either on the magma chamber floor or, if the floor was porous, below it on the compaction front, effectively isolating the underlying pyroxenite from the rocks above. Evidence that chromite and orthopyroxene coexisted in equilibrium and mechanically separated from each other comes from the fact that the Cr content of footwall orthopyroxene (average 0·43 wt % Cr_2O_3), which coexists with chromite, is identical to that of hanging wall orthopyroxene (average 0·44 wt % Cr_2O_3), even where the latter does not coexist with chromite.

Several aspects of this model need comment. First, if lavas and hypabyssal rocks are any indication, crystal-laden magmas are common (e.g. Marsh, 1996). Among the notable examples of phenocryst-bearing hypabyssal rocks are the Ferrar dolerite sills of Antarctica (Marsh, 2004), the Shonkin Sag laccolith of Montana (Hurlbut, 1939) and the peridotite dikes of southern Skye (Gibb, 1976). Furthermore, nearly all erupting calc-alkaline lavas and mid-ocean ridge basalts (MORBs) contain phenocrysts (including chromite in the case of MORB). Perhaps more immediately relevant are the peridotite sills that intruded the marginal rocks along the base of the eastern Bushveld Complex. Sharpe & Hulbert (1985) interpreted these rocks as crystal mushes formed in and injected from the Bushveld magma chamber. An alternative interpretation (Eales, 2000) is that they are samples of crystal mushes that were intruding into the Bushveld magma chamber.

Two obvious questions are: given what we know about natural magmatic systems, how much chromite-laden magma would have been necessary to form the UG2 chromitite, and is the amount geologically reasonable to account for the laterally extensive UG2 chromitite? Roeder *et al.* (2006) measured modal abundances of chromite of up to 0·15% in 22 MORB, Hawaiian, and Icelandic lavas, and in another well-studied example, Bannister *et al.* (1998) found the basaltic andesite of Paricutin, Mexico, to contain ≈0·04% chromite. To produce the UG2 chromitite and the mixed layer below it (equivalent to a 67 cm thick layer of pure chromite), a 447 m thick layer of a magma containing 0·15% chromite would have been necessary; if the magma contained 0·04% chromite, the required layer thickness would have been 1675 m. A 447 m thick layer spread over the $4.5 \times 10^4 \, km^2$ aereal extent of the Rustenburg Layered Series is equivalent to ≈$2 \times 10^4 \, km^3$ of magma. The ultramafic sills at the base of the eastern Bushveld (Sharpe & Hulbert, 1985) are relatively Cr-rich and must contain much more chromite than the lavas noted above. For example, sample CO-174 from the Zwakwater sill contains 0·84 wt % Cr_2O_3 (Sharpe & Hulbert, 1985, table 3). Assuming that sample CO-174 consists of 45% orthopyroxene and 5% clinopyroxene containing,

respectively, 0·5 and 0·9% Cr_2O_3 (Sharpe & Hulbert, 1985), the modal chromite (48% Cr_2O_3) content is ≈1·2%. If this sample is representative of the crystal mushes injected into the Bushveld chamber, then the required layer thickness is 56 m, corresponding to a magma volume of ≈$2.5 \times 10^3 \, km^3$. This volume is similar to that of individual lava flows of the Columbia River basalts (Reidel *et al.*, 1989). Therefore, these data indicate that the UG2 chromitite could have been produced by crystal accumulation from geologically reasonable amounts of magma.

As the magma originally contained both orthopyroxene and chromite in suspension, the minerals must have been mechanically sorted from each other. This may have occurred in the magma body, or it may also have occurred in a crystal slurry at the magma chamber floor; for example, by kinetic sieving. The latter process, which separates crystal populations of different size, has been suggested by Marsh (2004) to account for modal layering in one of the sills of the Ferrar dolerites. We have no observations that bear on how chromite and orthopyroxene may have been sorted.

The Sr (e.g. Hamilton, 1977; Kruger & Marsh, 1982; Sharpe, 1985; Kruger, 1994), Os (McCandless *et al.*, 1999; Schoenberg *et al.*, 1999), Pb (Harmer *et al.*, 1995; Mathez & Waight, 2003; Mathez & Kent, 2005), Nd (Maier *et al.*, 2000), and O (Schiffries & Rye, 1989; Harris *et al.*, 2005) isotopic signatures of Bushveld rocks all indicate that the Bushveld magmas include a crustal component. The O data are particularly interesting because they are remarkably uniform throughout most of the Bushveld Complex and imply that the magma contained a large proportion of crustal material. The present model also requires the presence of another crustal chamber. Furthermore, that chamber must have either assimilated enough material or been shallow enough to cool sufficiently to drive crystallization, while at the same time providing a semi-continuous source of magma to the body exposed at present.

Enrichment of the UG2 chromitite in PGEs

Much has been written about the origin of the PGE ores of the Bushveld Complex. The general model of Maier (2005) to account for the PGE enrichments associated with chromitites and the ultramafic portions of layered intrusions makes sense in the context of our model for the formation of the UG2 chromitite. The saturation of sulfur in mafic liquid is sensitive to the Fe content (e.g. Haughton *et al.*, 1974; Mathez, 1976), so fractionating crystalline phases that decrease Fe content will drive a magma to separate an immiscible sulfide–oxide melt. Among those phases are olivine and chromite. Both are early formed minerals in Bushveld-type magmas, so it is reasonable to assume that the magma that injected into the Bushveld chamber and led to the

formation of the UG2 chromitite contained droplets of PGE-bearing sulfide–oxide liquid as well as chromite in suspension. At the same time, decreasing pressure increases sulfur saturation in mafic liquids (Mavrogenes & O'Neill, 1999). Therefore, as the new magma batch ascended through the crust, the sulfide droplets partially dissolved in response to the decompression, increasing the PGE content of the residual sulfide liquid. The sulfide accumulated along with the chromite, and with cooling most of the sulfide reacted with chromite, leaving the PGEs enriched in the residual phases (Naldrett & Lehmann, 1988). This accounts for both the high PGE content of the UG2 chromitite and relative PGE abundances that are similar to those of sulfide-dominated PGE deposits but unlike abundance patterns of other chromitites (e.g. Peach & Mathez, 1996). [See Mathez (1999) and Maier (2005) for further discussion of the various models for the formation of PGE ores associated with chromitites.]

CONCLUSIONS

The fundamental assertion of this work is that the rocks above and below the UG2 chromitite were essentially identical when they first accumulated. This is also the case for another chromitite layer in Cameron's E unit in the Lower Critical Zone, and it is probably true as well for most of the other Bushveld chromitites, judging from Cameron's (1980, 1982) descriptions of stratigraphic sequence. This rules out chromitite formation by Irvine's (1977a) widely accepted mixing model, whatever its attraction to account for chromitites elsewhere, as well as all the other mixing models that have been proposed. It also rules out Lipin's (1993) pressure increase model because wholesale removal of chromite from the magma body is not recorded in any stratigraphic change in pyroxene Cr/Al ratio. The only conceivable ways that any of these models could be relevant to the UG2 chromitite is if the rock layers did not form in their present stratigraphic order, in which case a major portion of the model is missing, or if there has been extensive, post-accumulation modification of composition, for which evidence is currently lacking.

We propose a simple, new model whereby the Bushveld chromitites formed by accumulation of chromite from new batches of magma injected into the magma chamber and in which chromite crystals were suspended. The model is supported by the common observation of phenocrysts, including those of chromite, in lavas and hypabyssal bodies, and by chromite abundances in these and other rocks that suggest that geologically reasonable amounts of magma can account for even the massive UG2 chromitite. The model requires some crystallization to have occurred in a deeper chamber, for which there is ample geochemical evidence. Perhaps the Bushveld

Complex was the uppermost body of a whole sequence of crustal magma chambers reaching to the mantle, and this arrangement is what gives the Bushveld its unique character.

SUPPLEMENTARY DATA

Supplementary data for this paper are available at *Journal of Petrology* online.

REFERENCES

Asimow, P. D. & Ghiorso, M. S. (1998). Algorithmic modifications extending MELTS to calculate subsolidus phase relations. *American Mineralogist* **83**, 1127–1131.

Bannister, V., Roeder, P. & Poustovetov, A. (1998). Chromite in the Paricutin lava flows (1943–1952). *Journal of Volcanology and Geothermal Research* **87**, 151–171.

Barnes, S. J. (1986). The distribution of chromium among orthopyroxene, spinel and silicate liquid at atmospheric pressure. *Geochimica et Cosmochimica Acta* **50**, 1889–1909.

Cameron, E. N. (1977). Chromite in the central sector of the eastern Bushveld Complex, South Africa. *American Mineralogist* **62**, 1082–1096.

Cameron, E. N. (1980). Evolution of the lower Critical Zone, central sector, eastern Bushveld Complex, and its chromite deposits. *Economic Geology* **75**, 845–871.

Cameron, E. N. (1982). The Upper Citical Zone of the eastern Bushveld Complex—precursor of the Merensky Reef. *Economic Geology* **77**, 1307–1327.

Cameron, E. N. & Desborough, G. A. (1969). Occurrence and characteristics of chromite deposits—eastern Bushveld Complex. *Economic Geology Monograph* **4**, 23–40.

Campbell, I. H. & Murck, B. W. (1993). Petrology of the G and H chromitite zones in the Mountain View area of the Stillwater Complex, Montana. *Journal of Petrology* **34**, 291–316.

Cawthorn, R. G. & Walraven, F. (1998). Emplacement and crystallization time for the Bushveld Complex. *Journal of Petrology* **39**, 1669–1687.

Cawthorn, R. G., Davies, G., Clubley-Armstrong, A. & McCarthy, T. S. (1981). Sills associated with the Bushveld Complex, South Africa: an estimate of the parental magma composition. *Lithos* **14**, 1–15.

Cousins, C. A. & Feringa, G. (1964). The chromite deposits of the western belt of the Bushveld Complex. In: Haughton, S. H. (ed.) *The Geology of some Ore Deposits in Southern Africa*. Johannesburg: Geological Society of South Africa, pp. 183–202.

Davies, G., Cawthorn, R. G., Barton, J. M., Jr & Morton, M. (1980). Parental magma to the Bushveld Complex. *Nature* **287**, 33–35.

Eales, H. V. (1987). Upper Critical Zone chromitite layers at R.P.M. Union section mine, western Bushveld complex.

In: Stowe, C. W. (ed.) *Evolution of Chromium Ore Fields*. New York: Van Nostrand Reinhold, pp. 144–168.

Eales, H. V. (2000). Implications of the chromium budget of the Western Limb of the Bushveld Complex. *South African Journal of Geology* **103**, 141–150.

Eales, H. V. & Cawthorn, R. G. (1996). The Bushveld Complex. In: Cawthorn, R. G. (ed.) *Layered Intrusions*. Amsterdam: Elsevier, pp. 181–230.

Ford, C. E., Bigger, G. M., Humphries, D. J., Wilson, G., Dixon, D. & O'Hara, M. J. (1972). Role of water in the evolution of the lunar crust; an experimental study of sample 14310; an indication of lunar calc-alkaline volcanism. *Proceedings of the Third Lunar Science Conference. Geochimica et Cosmochimica Acta Supplement* **1**, 207–229.

Gaetani, G. A., Grove, T. L. & Bryan, W. B. (1994). Experimental phase relations of basaltic andesite from hole 839B under hydrous and anhydrous conditions. In: Hawkins, J., Parson, L. & Allan, J. (eds) *Proceedings of the Ocean Drilling Program: Scientific Results, 135*. College Station, TX: Ocean Drilling Program, pp. 557–563.

Ghiorso, M. S. & Sack, R. O. (1995). Chemical mass transfer in magmatic processes. IV. A revised and internally consistent thermodynamic model for the interpolation and extrapolation of liquid–solid equilibria in magmatic systems at elevated temperatures and pressures. *Contributions to Mineralogy and Petrology* **119**, 197–212.

Gibb, F. G. F. (1976). Ultrabasic rocks of Rhum and Skye: the nature of the parent magma. *Journal of the Geological Society, London* **132**, 209–222.

Hamilton, J. (1977). Isotope and trace element studies of the Great Dike and Bushveld mafic phase. *Journal of Petrology* **18**, 24–52.

Harmer, R. E., Auret, J. M. & Eglington, B. M. (1995). Lead isotope variations within the Bushveld Complex, southern Africa: a reconnaissance study. *Journal of African Earth Sciences* **21**, 595–606.

Harris, C., Pronost, J. J. M., Ashwal, L. D. & Cawthorn, R. G. (2005). Oxygen and hydrogen isotope stratigraphy of the Rustenburg layered suite, Bushveld Complex: Constraints on crustal contamination. *Journal of Petrology* **46**, 579–601.

Hatton, C. J. & von Gruenewaldt, G. (1987). The geological setting and petrogenesis of the Bushveld chromitite layers. In: Stowe, C. W. (ed.) *Evolution of Chromium Ore Fields*. New York: Van Nostrand Reinhold, pp. 109–143.

Haughton, D. R., Roeder, P. L. & Skinner, B. J. (1974). The solubility of sulfur in mafic magmas. *Economic Geology* **81**, 451–462.

Horan, M. F., Morgan, J. W., Walker, R. J. & Cooper, R. W. (2001). Re–Os isotopic constraints on magma mixing in the Peridotite Zone of the Stillwater Complex, Montana, USA. *Contributions to Mineralogy and Petrology* **141**, 446–457.

Hurlbut, C. S. (1939). Igneous rocks of the Highwood mountains, Montana. *Geological Society of America Bulletin* **50**, 1043–1112.

Irvine, T. N. (1975). Crystallization sequences in the Muskox intrusion and other layered intrusions—II. Origin of chromitite layers and similar deposits of other magmatic ores. *Geochimica et Cosmochimica Acta* **39**, 991–1020.

Irvine, T. N. (1977a). Origin of chromitite layers in the Muskox intrusion and other layered intrusions: a new interpretation. *Geology* **5**, 273–277.

Irvine, T. N. (1977b). Chromite crystallization in the join Mg_2SiO_4–$CaMgSi_2O_6$–$CaAl_2Si_2O_8$–$MgCr_2O_4$–SiO_2. *Carnegie Institution of Washington Yearbook* **76**, 465–472.

Irvine, T. N., Keith, D. W. & Todd, S. G. (1983). The J-M platinum–palladium Reef of the Stillwater complex, Montana, II. Origin by double-diffusive convective magma mixing and

implications for the Bushveld complex. *Economic Geology* **78**, 1287–1334.

Kinnaird, J. A., Kruger, F. J., Nex, P. A. M. & Cawthorn, R. G. (2002). Chromitites of the Bushveld Complex—processes of formation and PGE enrichment. *Economic Geology Research Institute, University of Witwatersrand, Information Circular Number* **369**, 26.

Kruger, F. J. (1994). The Sr-isotopic stratigraphy of the western Bushveld Complex. *South African Journal of Geology* **97**, 393–398.

Kruger, F. J. & Marsh, J. S. (1982). Significance of $^{87}Sr/^{86}Sr$ ratios in the Merensky cyclic unit of the Bushveld Complex. *Nature* **298**, 53–55.

Lambert, D. D., Walker, R. J., Morgan, J. W., Shirey, S. B., Carlson, R. W., Zientek, M. L., Lipin, B. R., Koski, M. S. & Cooper, R. L. (1994). Re–Os and Sm–Nd isotope geochemistry of the Stillwater Complex, Montana: Implications for the petrogenesis of the J-M Reef. *Journal of Petrology* **35**, 1717–1753.

Li, C., Ripley, E. M., Sarkar, A., Shin, D. & Maier, W. D. (2005). Origin of phlogopite–orthopyroxene inclusions in chromites from the Merensky Reef of the Bushveld Complex, South Africa. *Contributions to Mineralogy and Petrology* **150**, 119–130.

Lipin, B. R. (1993). Pressure increases in the formation of chromite seams and the development of the ultramafic series in the Stillwater complex, Montana. *Journal of Petrology* **34**, 955–976.

Longhi, J., Wooden, J. L. & Coppinger, K. D. (1983). The petrology of high-Mg dikes from the Beartooth Mountains, Montana: a search for the parent magma of the Stillwater Complex. *Journal of Geophysical Research Supplement* **88**, B53–B59.

Lorand, J.-P. & Ceuleneer, G. (1989). Silicate and base-metal sulfide inclusions in chromites from the Maqsad area (Oman ophiolite, Gulf of Oman): A model for entrapment. *Lithos* **22**, 173–190.

Maier, W. D. (2005). Platinum-group element (PGE) deposits and occurrences: mineralization styles, genetic concepts, and exploration criteria. *Journal of African Earth Sciences* **41**, 165–191.

Maier, W. D. & Eales, H. V. (1994). Plagioclase inclusions in orthopyroxene and olivine of the UG2–Merensky Reef interval: regional trends in the western Bushveld Complex. *South African Journal of Geology* **97**, 408–414.

Maier, W. D. & Teigler, B. (1995). A facies model for the western Bushveld Complex. *Economic Geology* **90**, 2343–2349.

Maier, W. D., Arndt, N. T. & Curl, E. A. (2000). Progressive crustal contamination of the Bushveld Complex: evidence from Nd isotopic analyses of the cumulate rocks. *Contributions to Mineralogy and Petrology* **140**, 316–327.

Marcantonio, F., Zindler, A., Reisberg, L. & Mathez, E. A. (1993). Re–Os isotopic systematics in chromitites from the Stillwater Complex, Montana, USA. *Geochimica et Cosmochimica Acta* **57**, 4029–4037.

Marsh, B. (1996). Solidification fronts and magmatic evolution. *Mineralogical Magazine* **60**, 5–40.

Marsh, B. (2004). A magmatic mush column rosetta stone: the McMurdo Dry Valleys of Antarctica. *EOS Transactions, American Geophysical Union* **85**, 497–502.

Martin, H. (1994). Archaean grey gneisses and the genesis of the continental crust. In: Condie, K. C. (ed.) *Archaean Crustal Evolution*. Amsterdam: Elsevier, pp. 205–259.

Mathez, E. A. (1976). Sulfur solubility and magmatic sulfides in submarine basalt glass. *Journal of Geophysical Research* **81**, 4269–4276.

Mathez, E. A. (1999). On factors controlling the concentrations of platinum group elements in layered intrusions and chromitites. In: Keays, R. R., Lesher, C. M., Lightfoot, P. D. &

Farrow, C. E. G. (eds), *Dynamic Processes in Magmatic Ore Deposits and their Application in Mineral Exploration. Geological Association of Canada Short Course Notes* **13**, 251–286..

Mathez, E. A. & Kent, A. J. R. (2005). Tracing geochemical evolution of the Bushveld Complex with lead isotopes analyzed by LA-MC-ICP-MS. *2005 Goldschmidt Conference Abstracts. Geochimica et Cosmochimica Acta* **69**, A331.

Mathez, E. A. & Mey, J. L. (2005). Character of the UG2 chromitite and host rocks and petrogenesis of its pegmatoidal footwall, northwestern Bushveld Complex. *Economic Geology* **100**, 1617–1630.

Mathez, E. A. & Waight, T. E. (2003). Lead isotopic disequilibrium between sulfide and plagioclase in the Bushveld Complex and the chemical evolution of large layered intrusions. *Geochimica et Cosmochimica Acta* **67**, 1875–1888.

Mathez, E. A., Hunter, R. H. & Kinzler, R. (1997). Petrologic evolution of partially molten cumulate: the Atok section of the Bushveld Complex. *Contributions to Mineralogy and Petrology* **129**, 20–34.

Maurel, C. & Maurel, P. (1982). Étude experimentale de la solubilité du chrome dans les bains silicatés basiques et de sa distribution entre liquide et minéraux coéxistants: conditions d'éxistence du spinelle chromifère. *Bulletin de Mineralogie* **105**, 640–647.

Mavrogenes, J. A., & O'Neill, H. St. C. (1999). The relative effects of pressure, temperature and oxygen fugacity on the solubility of sulfide in mafic magmas. *Geochimica et Cosmochimica Acta* **63**, 1173–1180.

McCandless, T. E., Ruiz, J., Adair, B. I. & Freydier, C. (1999). Re–Os isotope and Pd/Ru variations in chromitites from the Critical Zone, Bushveld Complex, South Africa. *Geochimica et Cosmochimica Acta* **63**, 911–923.

McElduff, B. & Stumpfl, E. F. (1991). The chromite deposits of the Troodox Complex, Cyprus: Evidence for the role of a fluid phase accompanying chromite formation. *Mineralium Deposita* **26**, 307–318.

McLaren, C. H. & De Villiers, J. P. R. (1982). The platinum-group chemistry and mineralogy of the UG2 chromitite layers of the Bushveld Complex. *Economic Geology* **77**, 1348–1366.

Melcher, F., Grum, W., Simon, G., Thalhammer, T. V. & Stumpfl, E. F. (1997). Petrogenesis of the ophiolitic giant chromite deposits of Kempirsai, Kazakhstan: a study of solid and fluid inclusions in chromite. *Journal of Petrology* **38**, 1419–1458.

Murck, B. N. & Campbell, I. H. (1986). The effects of temperature, oxygen fugacity and composition on the behavior of chromium in basic and ultramafic melts. *Geochimica et Cosmochimica Acta* **50**, 1871–1887.

Naldrett, A. J. & Lehmann, J. (1988). Spinel non-stoichiometry as an explanation for Ni-, Cu-, and PGE-enriched sulphides in chromitites. In: Prichard, H. M., Potts, P. J., Bowles, J. F. W. & Cribb, S. J. (eds) *Geo-platinum 87 Symposium*. Amsterdam: Elsevier, pp. 93–109.

Nicholson, D. M. & Mathez, E. A. (1991). Petrogenesis of the Merensky Reef in the Rustenburg section of the Bushveld Complex. *Contributions to Mineralogy and Petrology* **107**, 293–309.

Peach, C. L. & Mathez, E. A. (1996). Constraints on the formation of platinum group element deposits in igneous rocks. *Economic Geology* **91**, 439–450.

Raedeke, L. D. & McCallum, I. S. (1984). Investigations of the Stillwater Complex: Part II. Petrology and petrogenesis of the Ultramafic series. *Journal of Petrology* **25**, 395–420.

Reidel, S. P., Tolan, T. L., Hooper, P. R., Beeson, M. H., Fecht, K. R., Bentley, R. B. & Anderson, R. L. (1989). The Grande Ronde Basalt, Columbia River basalt group; stratigraphic descriptions and correlations in Washington, Oregon, and Idaho. In: Reidel, S. P. & Hooper, P. R. (eds) *Volcanism and Tectonism in the Columbia River Flood-Basalt Province. Geological Society of America, Special Papers* **239**, 21–54.

Roeder, P. L. & Reynolds, I. (1991). Crystallization of chromite and chromium solubility in basaltic melts. *Journal of Petrology* **32**, 909–934.

Roeder, P. L., Gofton, E. & Thornber, C. (2006). Cotectic proportions of olivine and spinel in olivine-tholeiitic basalt and evaluation of pre-eruptive processes. *Journal of Petrology* **47**, 883–900.

Schiffries, C. M. & Rye, D. M. (1989). Stable isotopic systematics of the Bushveld Complex: I. Constraints of magmatic processes in layered intrusions. *American Journal of Science* **289**, 841–873.

Schoenberg, R., Kruger, F. J., Nägler, T. F., Meisel, T. & Kramers, J. D. (1999). PGE enrichment in chromitite layers and the Merensky Reef of the western Bushveld Complex; a Re–Os and Rb–Sr isotope study. *Earth and Planetary Science Letters* **172**, 49–64.

Sen, G. & Presnall, D. C. (1984). Liquidus phase relationships on the join anorthite–forsterite–quartz at 10 kbar with applications to basalt petrogenesis. *Contributions to Mineralogy and Petrology* **85**, 404–408.

Sharpe, M. (1985). Strontium isotope evidence for preserved density stratification in the Main Zone of the Bushveld Complex, South Africa. *Nature* **316**, 119–126.

Sharpe, M. R. & Hulbert, L. J. (1985). Ultramafic sills beneath the Eastern Bushveld Complex: Mobilized suspensions of early Lower Zone cumulates in a parental magma with boninitic affinities. *Economic Geology* **80**, 849–871.

Sharpe, M. R. & Irvine, T. N. (1983). Melting relations of two Bushveld chilled margin rocks and implications for the origin of chromitite. *Carnegie Institution Geophysical Laboratory Yearbook* **82**, 295–300.

Sharpe, M. R., Irvine, T. N., Mysen, B. O. & Hazen, R. M. (1983). Density and viscosity characteristics of melts of Bushveld chilled margin rocks. *Carnegie Institution Geophysical Laboratory Yearbook* **82**, 300–305.

Sisson, T. W. & Grove, T. L. (1993). Experimental investigations of the role of H_2O in calc-alkaline differentiation and subduction zone magmatism. *Contributions to Mineralogy and Petrology* **113**, 143–166.

Spandler, C., Mavrogenes, J. & Arculus, R. (2005). Origin of chromitites in layered intrusions: Evidence from chromite-hosted melt inclusions from the Stillwater Complex. *Geology* **33**, 893–896.

Ulmer, G. C. (1969). Experimental investigations of chromite spinels. *Economic Geology Monograph* **4**, 114–131.

Wilson, A. H. (1992). The geology of the Great Dyke, Zimbabwe: crystallization, layering, and cumulate formation in the P1 Pyroxenite of Cyclic Unit 1 of the Darwendale subchamber. *Journal of Petrology* **33**, 611–663.